

# The Nearly Constant Loss, Johari-Goldstein $\beta$ -Relaxation, and $\alpha$ -Relaxation of 1,4-Polybutadiene

MARIA J. SCHROEDER,<sup>1</sup> KIA L. NGAI,<sup>2</sup> C. MICHAEL ROLAND<sup>2</sup>

<sup>1</sup>United States Naval Academy, Annapolis, Maryland 21402

<sup>2</sup>Naval Research Laboratory, Washington, District of Columbia 20375-5320

Received 8 August 2006; revised 2 November 2006; accepted 6 November 2006

DOI: 10.1002/polb.21051

Published online in Wiley InterScience (www.interscience.wiley.com).

**ABSTRACT:** From high-resolution dielectric spectroscopy measurements on 1,4-polybutadiene (1,4-PB), we show that in addition to the structural  $\alpha$ -relaxation and higher frequency secondary relaxations in the spectra, a nearly constant loss (NCL) is observed at shorter times/lower temperatures. The properties of this NCL are compared to those of another chemically similar polymer, 1,4-polyisoprene. The secondary relaxations in 1,4-PB include the well-known Johari-Goldstein (JG)  $\beta$ -relaxation and two other higher-frequency peaks. One of these, referred to as the  $\gamma$ -relaxation, falls between the JG-relaxation and the NCL. Seen previously by others, this  $\gamma$ -relaxation in 1,4-PB is not the JG-process and bears no relation to the glass transition. At very low temperatures (<15 K), we confirm the existence of a very fast secondary relaxation, having a weak dielectric strength and an almost temperature-invariant relaxation time. © 2006 Wiley Periodicals, Inc. *J Polym Sci Part B: Polym Phys* 45: 342–348, 2007

**Keywords:** dielectric properties; glass transition; polybutadiene; relaxation

## INTRODUCTION

The significance of the glass transition (i.e., structural relaxation or the  $\alpha$ -process) in liquids and polymers can hardly be understated. The cooperative dynamics of materials approaching vitrification has relevance to proteins (which exhibit features of glassy dynamics such as disorder, metastability, and freezing transitions), neural networks (neural learning can be modeled as a “cooling” process with different metastable structures), superconductors (“vortex glass transition”), and engineering polymers (sound attenuation and the skidding of tires on wet surfaces<sup>1</sup>). The glass transition is recognized as a major unsolved problem in condensed matter and accordingly has been the focus of experimental and theoretical efforts

for more than fifty years.<sup>2–4</sup> While structural relaxation receives most of the attention, there are other processes at higher frequency (or observed at lower temperatures).<sup>5–7</sup> Some of these reflect intramolecular degrees of freedom, involving specific chemical groups; such processes, especially common in polymers that have complex repeat units or large pendant groups,<sup>7</sup> are of less general interest. The slowest secondary relaxation is the Johari-Goldstein (JG) process, which seems to be universal.<sup>8,9</sup> It is of fundamental importance because it exhibits properties mimicking those of the  $\alpha$ -relaxation: a change from an Arrhenius T-dependence below  $T_g$  to a stronger T-dependence above  $T_g$ ; a change in the temperature dependence of the dielectric relaxation strength as  $T_g$  is traversed; a correlation of the JG-relaxation time and its activation energy with properties of the  $\alpha$ -relaxation. Thus, the JG-relaxation and the glass transition sense the thermodynamic state of the material in a qualitatively similar fashion. The parallel properties, together with the fact that the JG-relaxation

Correspondence to: M. J. Schroeder (E-mail: schroede@usna.edu)

*Journal of Polymer Science: Part B: Polymer Physics*, Vol. 45, 342–348 (2007)  
© 2006 Wiley Periodicals, Inc. \*This article is a US Government work and, as such, is in the public domain in the United States of America.

transpires prior to structural relaxation, leads to the idea that the former is the precursor to structural relaxation and  $T_g$ . If correct, an understanding of the glass transition requires an accounting of the behavior of the JG-relaxation.

At times shorter than  $\tau_{JG}$  (and most other secondary relaxations, if present) is the so-called nearly constant loss (NCL), which refers to a weakly frequency-dependent contribution to the loss<sup>10</sup>

$$\epsilon''_{NCL} \sim \omega^{-\lambda} \quad (1)$$

in which  $\lambda$  is a small positive exponent. Also present in the imaginary part of the susceptibility measured by light-scattering experiments<sup>11–14</sup> where it can give rise to a minimum at higher temperatures due to approach of the  $\alpha$ -process,<sup>15</sup> the NCL is a component of the dynamics of virtually all glass-forming liquids<sup>16</sup> as well as ionically-conducting materials.<sup>17–19</sup> In polymers prominent secondary relaxations limit observation of the NCL to a smaller range of frequencies; moreover, the level of the NCL decreases with decreasing temperature<sup>20</sup>

$$\epsilon''_{NCL}(T) \sim \exp(T/T_0) \quad (2)$$

making observation more difficult below  $T_g$ , where the NCL contributes in the frequency range of common dielectric spectrometers. Thus, while seen in light scattering measurements on polyisobutylene<sup>11</sup> and 1,4-polyisoprene (PI),<sup>21</sup> and several molecular liquids,<sup>12,22</sup> the only report to date of the NCL in dielectric spectra of amorphous polymers was for PI,<sup>23</sup> obtained using a high-precision bridge.

Our objective herein is to show the generality of the results for PI by making measurements on another polymer, 1,4-polybutadiene (1,4-PB). This choice is guided by the similar backbone structure of the two polydienes. However, notwithstanding its relatively simple chemical structure, the dynamics of 1,4-PB exhibits many interesting features. In addition to the glass transition and JG process, various other relaxations have been reported. Scattering experiments at  $\sim 20$  °C above  $T_g$  reveal three dynamic processes: at 19 ns from neutron spin echo spectroscopy,<sup>24</sup> at 2 ns by longitudinal Brillouin scattering,<sup>25</sup> and at 0.3 ns by depolarized Raman scattering.<sup>26</sup> The former two (slower) relaxations have been modeled by Colmenero et al. as atom hopping in an asymmetric double well potential.<sup>27</sup> The very short time relaxation seen in depolarized Raman measurements<sup>26</sup> was

also observed by Lusceac et al.<sup>28</sup> using dielectric and NMR spectroscopies. Lusceac et al.<sup>28</sup> have also reported an additional, very weak dielectric peak at  $T \sim 5$  K. We might also expect in principle the existence at shorter times of the “E-process” seen by quasielastic neutron scattering.<sup>29</sup>

In this work, we use broadband, high-resolution dielectric relaxation measurements under optimal conditions to show that the characteristic features of the dynamics of glass-forming materials are present in 1,4-PB. We analyze the properties of the JG relaxation and the NCL and find that, similar to results for PI and glass-forming liquids, the former bears a direct relationship to the glass transition. We also observe the two other secondary relaxations in 1,4-PB.

## EXPERIMENTAL

The polymer was a lithium-catalyzed medium *cis*-1,4 polybutadiene (8% vinyl content), obtained from A. F. Halasa of the Goodyear Tire and Rubber Co. It had a number average molecular weight = 560 kg/mol, polydispersity = 1.4, and  $T_g$  of about 181 K. Isothermal dielectric spectra were measured over the frequency range 10 Hz to 100 kHz using a special version (broader frequency range) of the Andeen-Hagerling 2700A capacitance bridge. The measurements employed a cell similar to that described elsewhere,<sup>23</sup> but with a solid 2-mm piece of brass used as the “high” electrode. This cell was mounted on the cold finger of a Precision Cryogenics dewar, and the temperature was controlled using a LakeShore Cryotronics DRC 82C temperature controller. Additional measurements were made using an IMass Inc. time domain dielectric spectrometer (frequency range from  $10^{-4}$  to  $10^4$  Hz) and a Novoccontrol Alpha Analyzer ( $10^{-2}$  to  $10^6$  Hz), in combination with a Delta Design 9023 liquid nitrogen-cooled oven. A parallel-plate geometry (25 mm diameter with sample thickness between 0.05 and 0.15 mm) with a guard ring on the detector side was employed for the latter. Samples were allowed to equilibrate at least 1 h after attaining the desired temperature, with replicate measurements used to assure thermal equilibration.

## RESULTS AND DISCUSSION

There are at least four dielectric processes in 1,4-PB, as exemplified in Figure 1, showing the

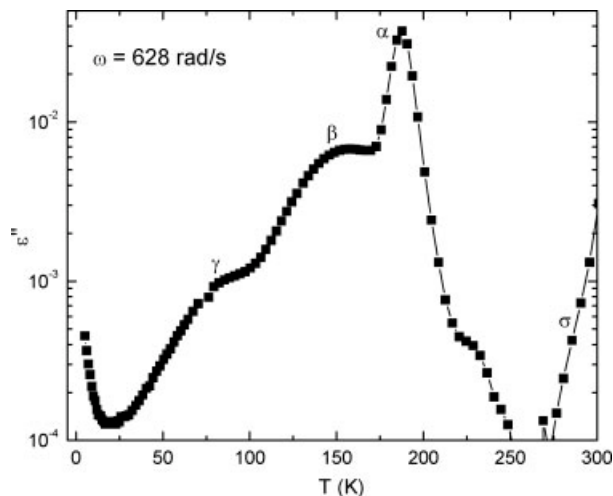


**Figure 1.** Temperature dependence of the dielectric loss of 1,4-PB, with the various dispersions indicated.

dielectric loss measured at 100 Hz as a function of temperature. At the highest temperatures there is a d.c.-conductivity contribution,  $\sigma$ , from mobile ions, followed by the prominent  $\alpha$ -peak reflecting the glass transition (local segmental relaxation). Toward lower temperatures are the JG-process, in proximity to the  $\alpha$ -peak and having substantial dielectric strength, and a  $\gamma$ -secondary relaxation. The NCL becomes apparent as a linear slope of the data at temperatures below the  $\gamma$ -peak. At still lower temperatures, but not discernible in Figure 1, is a very weak peak, first discovered by Lusceac et al.<sup>28</sup> Each of these features in the spectrum is considered below.

#### Isothermal Data at Temperatures Above $T_g$ : $\alpha$ - and JG-Relaxations

Figure 2 shows a representative loss spectrum at a temperature (173.8 K) for which both the  $\alpha$ -relaxation and the JG-process (also referred to as the  $\beta$ -relaxation by Lusceac et al.<sup>28</sup>) fall within the experimental window. The  $\alpha$ -peak can be fit to the one-sided Fourier transform of the KWW function

$$\varepsilon''(\omega) = \Delta\varepsilon \int_0^\infty dt \left[ \frac{-d}{dt} \exp - (t/\tau_{\text{KWW}})^{\beta_{\text{KWW}}} \right] \sin(\omega t) \quad (3)$$

with  $\beta_{\text{KWW}} = 0.47$  and  $\tau_{\text{KWW}} = 0.724\tau_\alpha$  for this value of  $\beta_{\text{KWW}}$  ( $\tau_\alpha = (\omega_{\text{max}})^{-1}$  where  $\omega_{\text{max}}$  is the circular frequency of the peak maximum). The value of the exponent is somewhat smaller

(broader peak) than the  $\beta_{\text{KWW}} = 0.50$  deduced from mechanical and dielectric relaxation measurements on 1,4-PB having a lower molecular weight and slightly different chemical structure (i.e., lower vinyl content).<sup>30</sup> The breadth of the  $\alpha$ -peak in polybutadiene is a strong function of the relative concentration of 1,2- and 1,4-units in the polybutadiene backbone,<sup>31</sup> with the narrowest breadth seen in 1,4-PB. This material is a “strong” polymer (in the Angell sense<sup>32</sup>), with a  $T_g$ -normalized Arrhenius slope for the  $\alpha$ -relaxation times,  $\frac{T_g d \log \tau_\alpha}{dT^{-1}}$ , measured to be 93.

Empirically, it is found that the ratio of the  $\alpha$ -relaxation time,  $\tau_\alpha$ , to the JG relaxation time,  $\tau_{\text{JG}}$ , is correlated with the breadth of the  $\alpha$ -relaxation peak,<sup>33</sup>

$$\log \tau_\alpha - \log \tau_{\text{JG}} = (1 - \beta_{\text{KWW}})(\log \tau_\alpha - \log t_c) \quad (4)$$

where  $t_c$  is a constant ( $= 2$  ps). For  $\tau_\alpha = 285$  s (the spectra in Fig. 2), eq 4 yields  $\tau_{\text{JG}} = 8.98 \times 10^{-6}$  s. The frequencies corresponding to these relaxation times are indicated by the arrows in Figure 2. The calculated  $\omega_{\text{JG}}$  is roughly consistent with the observed JG maximum. Note that the latter is only clearly discerned after removal of the contribution to  $\varepsilon''$  from the cable resistance. This was measured separately, then the

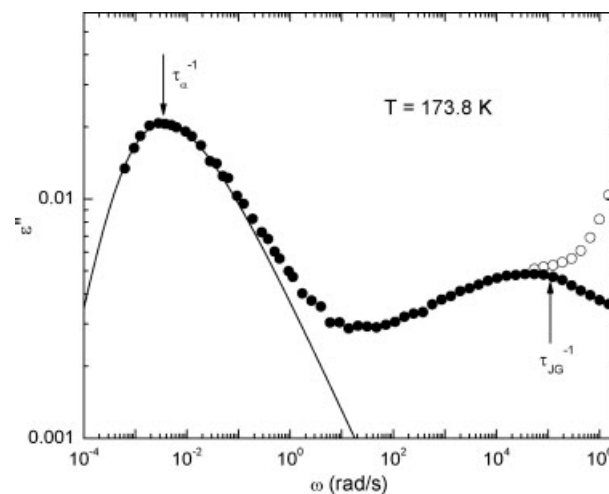


**Figure 2.** Dielectric loss at 173.8 K showing the local segmental relaxation and JG dispersions. The rise at higher frequencies due to cable resistance (denoted by the hollow symbols) was removed (see text) to reveal the underlying secondary dispersion. The arrows indicate the frequency of the  $\alpha$ -peak and the predicted frequency (eq 4) of the JG peak.

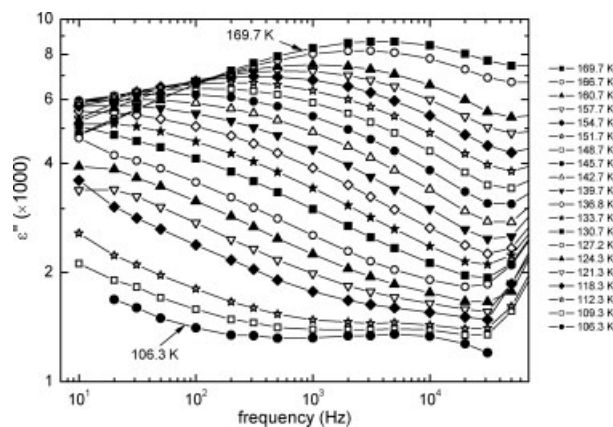


**Figure 3.** Dielectric loss over a range of temperatures for which the JG peak dominates the measured response. The temperatures follow the order listed in the legend.

respective impedances for the sample and cable were subtracted,<sup>34</sup> with the dielectric loss in Figure 2 calculated from the difference.

At temperatures higher than in Figure 2, the JG-peak begins to encroach on the  $\alpha$ -relaxation, making determination of the relaxation times less accurate, especially given the substantial relaxation strength of the JG process in 1,4-PB. This merging contributes to an apparent broadening and anomalous increase of the width of the main loss peak with increasing temperature.<sup>30</sup> Various methods to deconvolute these overlapping dispersions have been proposed; however, all are specific to a particular interpretation of the JG-process.<sup>35–37</sup>

#### Isothermal Data at Temperatures Below $T_g$ : JG- and $\gamma$ -Relaxations

Figure 3 shows the dielectric loss over a range of temperatures indicated in the figure for which the  $\alpha$ -process has become too slow to be observed, so that the JG-peak is prominent in the measured frequency range. The peak maxima for the nine highest temperatures, from 142.7 to 169.7 K, lie within the experimental frequency window and their frequencies can be determined unambiguously without use of any fitting procedure. From the frequencies of the peak maxima we obtain the most probable JG-relaxation times in this temperature range and the results are shown in Figure 4. The usual Arrhenius behavior is observed below  $T_g$ , with an activation energy,  $E_{JG} = 35.9 \pm 0.6$  kJ/mol. This is comparable to previously reported values for 1,4-PB, in the range from 34 to 38 kJ/mol.<sup>38–40</sup>

*Journal of Polymer Science: Part B: Polymer Physics*  
DOI 10.1002/polb

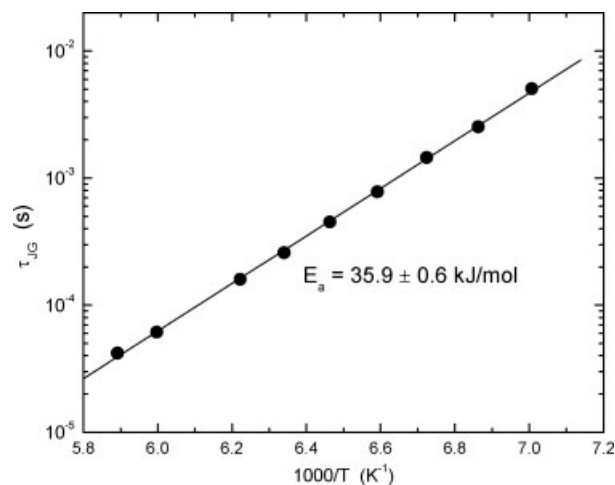


**Figure 4.** Arrhenius plot of the JG relaxation times, yielding the indicated value for the activation energy.

At the lower temperatures in Figure 3 another secondary peak (“ $\gamma$ -process”) appears; this was first reported by Lusceac et al. from dielectric and  $^2\text{H}$ -NMR measurements on similar polybutadienes.<sup>28</sup> As the temperature is reduced further (Fig. 5) to  $107 > T$  (K)  $> 82$ , the  $\gamma$ -peak becomes dominant in the measured frequency range. To extract its relaxation time,  $\tau_\gamma$ , from the spectra, the contribution from the slower JG peak was fit to a power law, which in turn was subtracted from the spectrum. The resulting deconvoluted  $\gamma$ -peak was then fit to a Cole-Cole function<sup>6</sup>

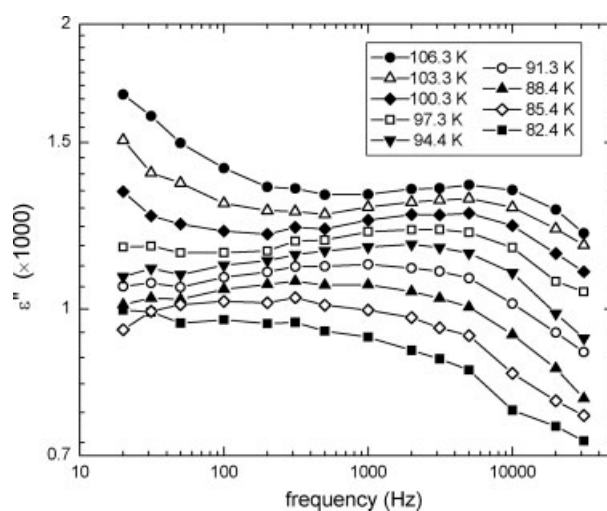


**Figure 5.** Dielectric loss over a range of temperatures for which the  $\gamma$ -peak is prominent in the measured spectrum.

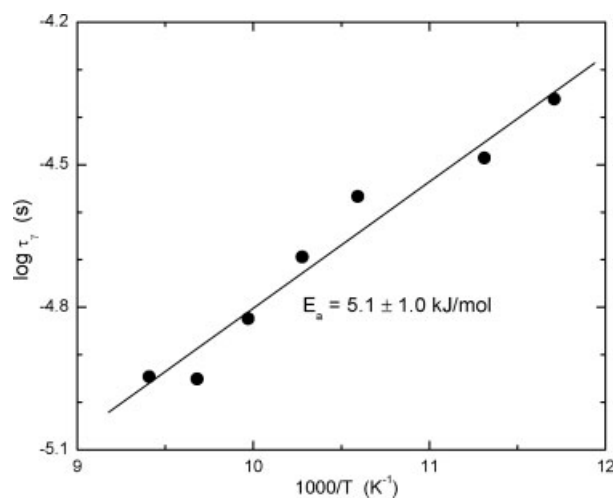


**Figure 6.** Arrhenius plot of the  $\gamma$ -relaxation times, yielding the indicated value for the activation energy.

$$\varepsilon''(\omega) = \Delta\varepsilon \frac{(\omega\tau)^\beta \sin(\beta\frac{\pi}{2})}{1 + 2(\omega\tau)^\beta \cos(\beta\frac{\pi}{2}) + (\omega\tau)^{2\beta}} \quad (5)$$

The resulting  $\tau_\gamma$  values are plotted in Figure 6, revealing an Arrhenius temperature dependence with an activation energy,  $E_a \sim 5$  kJ/mol. Lusceac et al.<sup>28</sup> had found that their 1,4-PB samples, which had small variations in chemical structure, exhibited a range of activation energies for the  $\gamma$ -relaxation,  $11 < E_a$  (kJ/mol)  $< 20$ ; moreover, there was no obvious relationship between the polymer and its  $E_a$ . The highest molecular weight sample (80 kg/mol) studied by Lusceac et al.<sup>28</sup> had the highest  $E_a$ , although there was no general correlation between  $M_w$  and  $E_a$ . Ding et al.<sup>26</sup> observed a secondary relaxation in 1,4-PB by depolarized light scattering that was not the (JG)  $\beta$ -relaxation and had a similar activation energy of 15 kJ/mol. This  $E_a$  is close to that found in simulations for rotations involving the backbone vinyl carbons in 1,4-PB.<sup>41,42</sup>

From Brillouin and X-ray scattering on 1,4-PB, Fioretto et al.<sup>43</sup> identified a secondary process, distinct from the JG-relaxation, having an activation energy = 7.2 kJ/mol. This is comparable to the  $E_a$  found herein for the  $\gamma$ -peak. The value is close to the barrier to torsional motion of the 1,4-PB backbone, as determined by simulations.<sup>42,44</sup>

#### Isothermal Data at Temperatures Below 83 K: Nearly Constant Loss

At still lower temperatures, the  $\gamma$ -relaxation moves to lower frequencies whereby the NCL

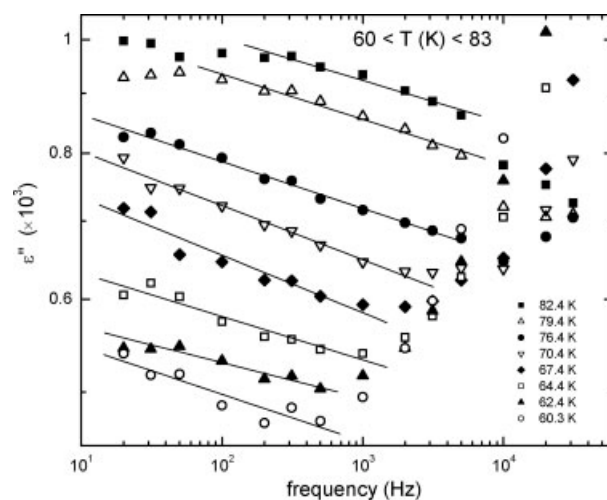


**Figure 7.** Dielectric spectra at temperatures over which loss can be approximated by a weak power law dependence, eq 1 with  $\lambda = 0.04$ .

becomes apparent in the spectra. It can be seen in Figure 7 as a contribution on the low frequency side of the  $\gamma$ -peak at higher temperatures, encompassing most of the spectral range at the lowest temperatures in the figure. The NCL can be fitted to eq 1 with  $\lambda = 0.04 \pm 0.006$ , as indicated by the solid lines. This frequency dependence,  $\omega^{-0.04}$ , is weaker than for PI as reported by Sokolov et al.<sup>11</sup> from light scattering,  $\omega^{-0.15}$ . The magnitude of the NCL for 1,4-PB is plotted versus temperature in Figure 8 with the fit to eq 2 giving  $T_0 = 32.3$  K. This is significantly smaller than for PI, for which  $T_0 = 79.8$  K<sup>23</sup>, meaning that the NCL changes more rapidly with temperature for 1,4-PB than for PI.

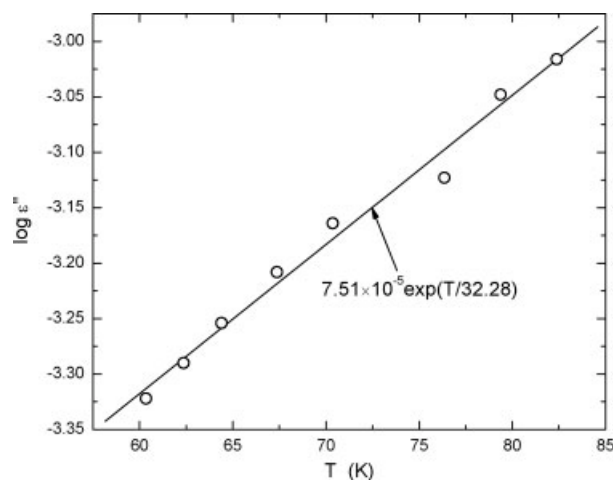


**Figure 8.** Temperature dependence of the NCL data of Figure 7, along with the fit to eq 2.

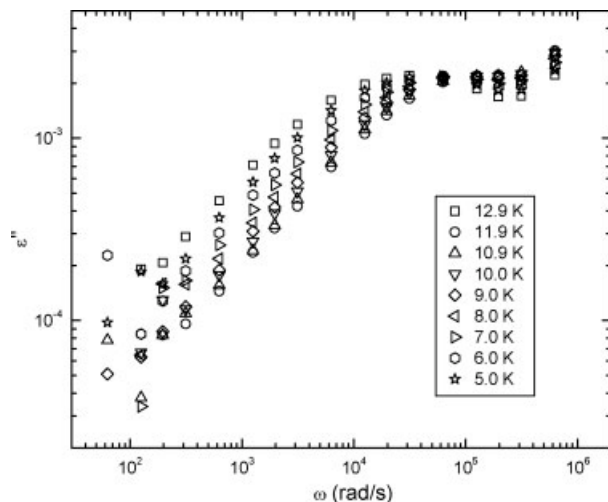


**Figure 9.** Low temperature loss spectra showing the T-insensitive peak.

### Below the NCL Regime

The negligible temperature dependence below 1 K of amorphous solids is explained by degenerate configurations for small groups of atoms, described to a good approximation by a double-well potential with parameters widely distributed due to the irregular structure of these materials. Quantum tunneling enables oscillations of atoms between the two configurations, giving rise to a linear specific heat.<sup>45</sup> At higher temperatures ( $> \sim 5$  K), the heat capacity and other properties deviate from the predictions of the simple two-level tunneling model due to breakdown of the two-level description and the contribution of incoherent tunneling arising from overdamped two-level systems.<sup>46</sup> In Figure 9 below about 15 K, 1,4-PB exhibits a very weak peak at about 2 kHz. Lusceac et al.<sup>28</sup> reported a similar finding in their polybutadiene samples. Although the data are too sparse to allow any quantitative analysis, there appears to be negligible temperature sensitivity. This is consistent with quantum tunneling behavior.

## CONCLUSIONS

Among the secondary relaxations found in 1,4-PB, the  $\beta$ -relaxation is closest to the  $\alpha$ -relaxation and, unlike the faster  $\gamma$ -process, merges with the  $\alpha$ -relaxation at higher temperatures. The respec-

tive  $\alpha$ - and  $\beta$ -relaxation times in 1,4-PB are consistent with the latter being the JG-process and thus functions as the precursor to structural relaxation. As noted by Lusceac et al.<sup>28</sup>  $\tau_\beta$  values are insensitive to molecular weight after temperature is normalized to  $T_g$ ; this follows from the relationship between the  $\alpha$ - and JG  $\beta$ -relaxation times (eq 4, assuming the  $\beta_{KWW}$  exponent is independent of molecular weight) and is consistent with the results in Figure 2.

Following these two secondary processes is a region over which the loss changes only very weakly. This NCL has properties similar to those seen previously for PI.<sup>23</sup> One source of the NCL is relaxation of segments while they are still caged at times much shorter than the structural segmental relaxation. This NCL is also seen in ionic conductors<sup>17–19</sup> and its origin is relaxation of caged ions at times long before the ions execute local and long range diffusion that give rise to a.c. and d.c. conductivity.<sup>18,19</sup> Indeed, the ions giving rise to the  $\sigma$  in Figure 1 may also contribute to the NCL. This contribution is likely quite small, however, since we only observe the d.c. conductivity at low frequencies. Any a.c. conductivity at higher frequencies is swamped by the strong  $\alpha$ -relaxation dynamics, and similarly, we expect the NCL due to ion motion at still higher frequencies to be relatively small. Experiments involving the addition (or removal) of ions to the 1,4-PB could quantify their effect (if any) on the magnitude of the NCL, but such work is beyond the scope of the present study.

Below the NCL another secondary peak emerges; however, its negligible temperature dependence makes it only observable at very low temperatures approaching 0 K. The origin of this weak contribution to the dielectric response is unknown, but the invariance to temperature is consistent with a tunneling mechanism.

This work was supported by the Office of Naval Research. We thank E.A. Rössler for providing his data in electronic format and J.J. Fontanella for assistance with some of the dielectric measurements in this article.

## REFERENCES AND NOTES

1. Roland, C. M. *Rubber Chem Technol* 2006, 79, 429.
2. Roland, C. M.; Hensel-Bielowka, S.; Paluch, M.; Casalini, R. *Rep Prog Phys* 2005, 68, 1405.

3. (a) Proceedings of the Third International Discussion Meeting on Relaxation in Complex Systems. *J Non-Cryst Solids* 1998, 235–237; (b) Proceedings of the Fourth International Discussion Meeting on Relaxation in Complex Systems. *J Non-Cryst Solids* 2002, 307–310.
4. Angell, C. A.; Ngai, K. L.; McKenna, G. B.; McMillan, P. F.; Martin, S. W. *J Appl Phys* 2000, 88, 3113.
5. Lunkenheimer, P.; Schneider, U.; Brand, R.; Loidl, A. *Contemp Phys* 2000, 41, 15.
6. Broadband Dielectric Spectroscopy; Kremer, F.; Schönhals, A., Eds.; Springer-Verlag: Berlin, 2003.
7. McCrum, N. G.; Read, B. E.; Williams, G. *Anelastic and Dielectric Effects in Polymer Solids*; Wiley: London, 1967.
8. Casalini, R.; Roland, C. M. *Phys Rev Lett* 2003, 91, 15702.
9. Ngai, K. L.; Paluch, M. *J Chem Phys* 2004, 120, 857.
10. Jonscher, A. K. *Dielectric Relaxation in Solids*; Chelsea Dielectric Press: London, 1983.
11. Sokolov, A. P.; Kisliuk, A.; Novikov, V. N.; Ngai, K. L. *Phys Rev B* 2001, 63, 172204.
12. Surovtsev, N. V.; Adichtchev, S. V.; Wiedersich, J.; Novikov, V. N.; Rössler, E. A. *J Chem Phys* 2003, 119, 12399.
13. Casalini, R.; Ngai, K. L.; Roland, C. M. *J Chem Phys* 2000, 112, 5181.
14. Casalini, R.; Ngai, K. L. *J Non-Cryst Solids* 2001, 293, 318.
15. Ngai, K. L.; Casalini, R. *Phys Rev B*, 2002, 66 2002, 132205.
16. Ngai, K. L. *J Phys Condens Matter* 2003, 15, S1107.
17. Lunkenheimer, P. *Dielectric Spectroscopy of Glass Dynamics*; Shaker: Aachen, 1999.
18. Ngai, K.L.; Leon, C. *Phys Rev B* 2002, 66, 064308.
19. Habasaki, J.; Ngai, K.L.; Hiwatari, Y. *Phys Rev B* 2002, 66, 021205.
20. Kudlik, A.; Benkhof, S.; Blochowicz, T.; Tschirwitz, C.; Rössler, E. *Mol Struct* 1999, 479, 210.
21. Sokolov, A. P., unpublished.
22. Cang, H.; Novikov, V. N.; Fayer, M. D. *J Chem Phys* 2003, 118, 2800.
23. Roland, C. M.; Schroeder, M. J.; Fontanella, J. J.; Ngai, K. L. *Macromolecules* 2004, 37, 2630.
24. Arbe, A.; Richter, D.; Colmenero, J.; Farago B. *Phys Rev E* 1996, 54, 3853.
25. Aouadi, A.; Lebon, M. J.; Dreyfus, C.; Strube, B.; Steffen, W.; Patkowski, A.; Pick, R. M. *J Phys Condens Matter* 1997, 9, 3803.
26. Ding, Y.; Novikov, V. N.; Sokolov, A. P. *J Polym Sci Part B: Polym Phys* 2004, 42, 94.
27. Colmenero, J.; Arbe, A.; Alvarez, F.; Narros, A.; Monkenbusch, M.; Richter, D. *Europhys Lett* 2005, 71, 262.
28. Lusceac, S. A.; Gainaru, C.; Vogel, M.; Koplin, C.; Medick, P.; Rössler, E. A. *Macromolecules* 2005, 38, 5625.
29. Kanaya, T.; Kaji, K. *Adv Polym Sci* 2001, 88, 154.
30. Robertson, C. G.; Roland, C. M. *Macromolecules* 2000, 33, 1262.
31. (a) Roland, C. M.; Ngai, K. L. *Macromolecules* 1991, 24, 5315; (b) Roland, C. M.; Ngai, K. L. *Macromolecules* 1992, 25, 1844.
32. Böhmer, R.; Ngai, K. L.; Angell, C. A.; Plazek, D. J. *J Chem Phys* 1993, 99, 4201.
33. Ngai, K. L. *J Chem Phys* 1998, 109, 6982.
34. Edwards, D. D.; Hwang, J. H.; Ford, S. J.; Mason, T. O. *Solid State Ionics* 1997, 99, 85.
35. Arbe, A.; Richter, D.; Colmenero, J.; Farago, B. *Phys Rev E* 1996, 54, 3853.
36. Williams, G.; Watts, D. C. In *NMR Basic Principles and Progress*; Dielh, P.; Fluck, E.; Kosfeld, R., Eds.; Springer: Berlin, 1971; Vol. 4, p 271.
37. Donth, E.; Schroter, K.; Kahle, S. *Phys Rev E* 1999, 60, 1099.
38. Hofmann, A.; Alegria, A.; Colmenero, J.; Willner, L.; Buscaglia, E.; Hadjichristidis, N. *Macromolecules* 1996, 29, 129.
39. Deegan, R. D.; Nagek. S. R. *Phys Rev B* 1995, 52, 5653.
40. Cervený, S.; Bergman, R.; Schwartz, G. A.; Jacobsson, P. *Macromolecules* 2002, 35, 4337.
41. Kim, E. G.; Mattice, W. L. *J Chem Phys* 2002, 117, 2389.
42. Gee, R. H.; Boyd, R. H. *J Chem Phys* 1994, 101, 8028.
43. Fioretto, D.; Masciovecchio, C.; Mattarelli, M.; Monaco, G.; Palmieri, L.; Ruocco, G.; Sette, F. *Philo Mag B* 2002, 82, 273.
44. Aoudi, A.; Lebon, M. J.; Dreyfus, C.; Strube, B.; Steffen, W.; Patkowski, A.; Pick, R. M. *J Phys Condens Matter* 1997, 9, 2803.
45. *Topics in Current Physics, Vol. 24: Amorphous Solids*; Phillips, W. A., Ed.; Springer: Berlin, 1984.
46. Rau, S.; Enss, C.; Hunklinger, S.; Neu, P.; Wurger, A. *Phys Rev B* 1995, 52, 7179.